Imatinib Mesylate Inhibits Proliferation and Exerts an Antifibrotic Effect in Human Breast Stroma Fibroblasts

Vassiliki Gioni,[1] Theodoros Karampinas,[1] Gerassimos Voutsinas,[2] Andreas E. Roussidis,[3] Savvas Papadopoulos,[4] Nikos K. Karamanos,[3] and Dimitris Kletsas[1]

[1]Laboratory of Cell Proliferation and Ageing and [2]Laboratory of Environmental Mutagenesis and Carcinogenesis, Institute of Biology, NCSR "Demokritos"; [3]Department of Pathology, "Hygeia" Hospital, Athens, Greece and [4]Department of Chemistry, Laboratory of Biochemistry, University of Patras, Patras, Greece

Abstract

Tumor stroma plays an important role in cancer development. In a variety of tumors, such as breast carcinomas, a desmoplastic response, characterized by stromal fibroblast and collagen accumulation, is observed having synergistic effects on tumor progression. However, the effect of known anticancer drugs on stromal cells has not been thoroughly investigated. Imatinib mesylate is a selective inhibitor of several protein tyrosine kinases, including the receptor of platelet-derived growth factor, an important mediator of desmoplasia. Recently, we have shown that imatinib inhibits the growth and invasiveness of human epithelial breast cancer cells. Here, we studied the effect of imatinib on the proliferation and collagen accumulation in breast stromal fibroblasts. We have shown that it blocks the activation of the extracellular signal-regulated kinase and Akt signaling pathways and up-regulates cyclin-dependent kinase inhibitor p21^{WAF1}, leading to the inhibition of fibroblast proliferation, by arresting them at the G_0/G_1 phase of the cell cycle. Imatinib inhibits more potently the platelet-derived growth factor–mediated stimulation of breast fibroblast proliferation. By using specific inhibitors, we have found that this is due to the inhibition of the Akt pathway. In addition, imatinib inhibits fibroblast-mediated collagen accumulation. Conventional and quantitative PCR analysis, as well as gelatin zymography, indicates that this is due to the down-regulation of mRNA synthesis of *collagen I* and *collagen III*—the main collagen types in breast stroma—and not to the up-regulation or activation of collagenases matrix metalloproteinase 2 and matrix metalloproteinase 9. These data indicate that imatinib has an antifibrotic effect on human breast stromal fibroblasts that may inhibit desmoplastic reaction and thus tumor progression. (Mol Cancer Res 2008;6(5):706–14)

Received 7/27/07; revised 12/20/07; accepted 1/16/08.

Grant support: Greek National Central Council of Health (KESY).

The costs of publication of this article were defrayed in part by the payment of page charges. This article must therefore be hereby marked *advertisement* in accordance with 18 U.S.C. Section 1734 solely to indicate this fact.

Requests for reprints: Dimitris Kletsas, Laboratory of Cell Proliferation and Ageing, Institute of Biology, National Center for Scientific Research "Demokritos," 153 10 Athens, Greece. Phone: 210-6503565; Fax: 210-6511767. E-mail: dkletsas@bio.demokritos.gr

doi:10.1158/1541-7786.MCR-07-0355

Introduction

As the majority of human malignancies is epithelial carcinomas, the main anticancer research effort has been directed against these neoplastic cells. However, cancer cells do not act alone, but rather coexist with their specific microenvironment. Tumor stroma contains many cell types, most important of which are fibroblasts, which, via the secretion of extracellular matrix components, growth factors, and proteases, affect crucially tumor development (1-4). In many solid tumors, predominately in the breast, carcinomas are characterized by a specific stromal reaction called desmoplasia, often referred to as scirrhous carcinoma (2, 5). This reaction is classically described by the proliferation of fibroblasts adjacent to the tumor and the overproduction of extracellular matrix components, mainly collagen. Moreover, it has been shown in human breast carcinomas that the major initiator of tumor desmoplasia is platelet-derived growth factor (PDGF) secreted by cancer cells and acting in a paracrine manner on stromal fibroblasts (6). Finally, this reaction exhibits synergistic effects on breast carcinoma progression (6), whereas carcinomas bearing desmoplastic stroma are associated with poor prognosis (7, 8).

Tumor stroma fibroblasts (termed "activated fibroblasts" or "cancer-associated fibroblasts"), although they share many morphologic and functional similarities with fibroblasts from other locations and pathologic conditions, exhibit a distinct gene expression profile (1, 9). In particular, they express a "myofibroblast" phenotype characterized by the concurrent expression of α-smooth muscle actin and vimentin, stress fibers, and a prominent rough endoplasmatic reticulum, among others (1). The origin of these cells is still a matter of debate, as it has been proposed that these myofibroblasts can be recruited from residential fibroblasts (10), from circulating CD-34–positive cells (11), or from epithelial tumor cells after an epithelial-mesenchymal transition (12). However, although the importance of stromal cells in tumor development is now supported by clinical studies and other experimental models (13-15), the effect of known anticancer drugs on these cells has not been thoroughly investigated.

Imatinib mesylate (also known as Gleevec or STI571) is a 2-phenylaminopyrimidine derivative that is a competitor of ATP and inhibits specific tyrosine kinases, such as Brc-Abl (the leading cause of chronic myelogenous leukemia), as well as c-Kit and PDGF receptors, which regulate major cellular events in several solid tumors (16). A number of studies have shown an inhibitory effect of imatinib on the growth of a variety of tumor cell types, such as of myeloid, lung, thyroid,

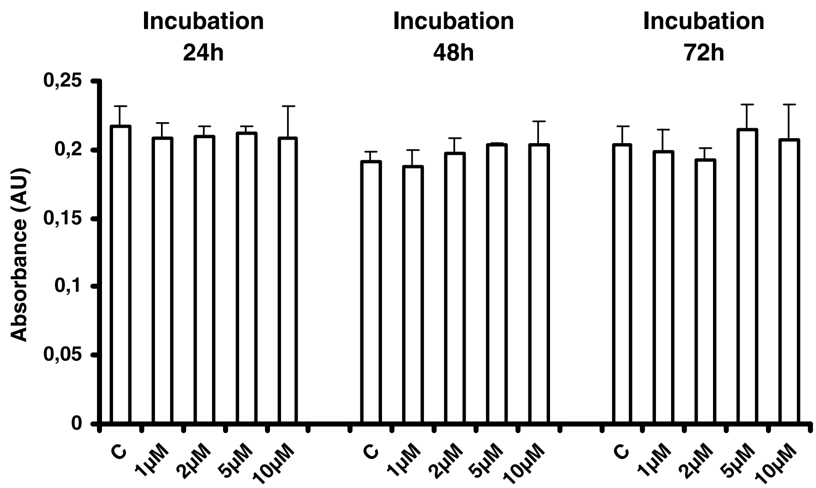

FIGURE 1. Effect of imatinib mesylate on the viability of human breast stromal fibroblasts. Cells were grown until confluency and were then incubated for 24, 48, or 72 h in the presence of the indicated concentrations of imatinib. Cell viability was then estimated with an MTT assay. Each point represents the average of four wells. One representative of three similar experiments is shown here.

pancreatic, osteosarcoma, or ovarian origin (17-24). In addition, it is currently used for the treatment of chronic myelogenous leukemia and gastrointestinal stromal tumors (25, 26). Recently, we have shown that imatinib inhibits also the proliferation and invasiveness of a panel of human epithelial breast cancer cells with different invasion potential (27, 28). So, having in mind that breast carcinomas are often characterized by a desmoplastic stromal reaction and the role of the latter in cancer growth, we studied the effect of imatinib on the proliferation of human breast fibroblasts and the production of collagen, as well as the molecular mechanisms underlying these events.

Results

Imatinib Inhibits the Proliferation of Human Breast Fibroblasts

First, we studied the effect of imatinib on the viability of human breast fibroblasts. Confluent cultures of fibroblasts in the presence of serum were incubated with increasing concentrations of imatinib up to 10 μmol/L for a 1-day, 2-day, or 3-day period, and cytotoxicity was measured by using the 3-(4,5-dimethylthiazol-2-yl)-2,5-diphenyltetrazolium bromide (MTT) assay. As shown in Fig. 1, even at a concentration of 10 μmol/L, imatinib had no effect on fibroblast viability. Interestingly, imatinib had also no cytotoxic effect on fibroblasts growing in the absence of serum (not shown). Subsequently, the effect of imatinib on the proliferation of breast fibroblasts was investigated. In subconfluent fibroblast cultures, in the presence of serum, increasing concentrations of imatinib from 0.1 to 10 μmol/L were added and novel DNA synthesis was estimated after a 24-hour incubation by measuring [^{3}H]thymidine incorporation. As can be seen in Fig. 2A, imatinib inhibited fibroblast proliferation in a dose-dependent manner; a slight inhibition can be observed also from the lowest concentration used, i.e., 0.1 μmol/L, and IC_{50} was ~1 μmol/L. Cell cycle analysis of imatinib-treated cells, done by flow cytometry, revealed a significant, dose-dependent decrease in S phase and an accumulation of cells in the G_0/G_1 phase; no obvious alterations in the proportion of the G_2/M phase were observed (Fig. 2B). In addition, we have not

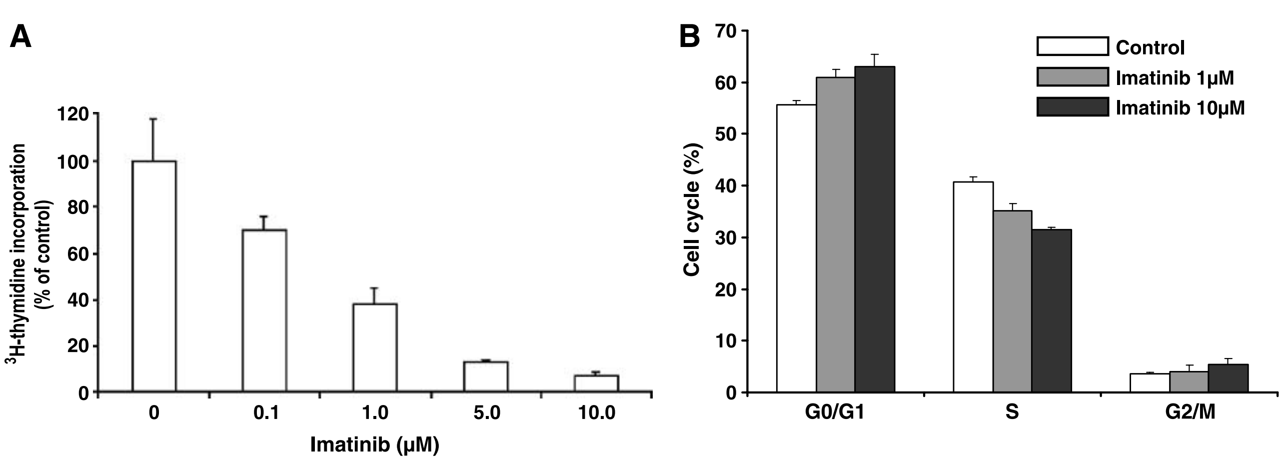

FIGURE 2. Imatinib mesylate inhibits the proliferation of human breast stromal fibroblasts. **A.** Subconfluent fibroblast cultures, grown in DMEM supplemented with 10% FCS, were treated with the indicated concentrations of imatinib in the presence of tritiated thymidine (0.1 μCi/mL). At 24 h after treatment, DNA synthesis was estimated as described in Materials and Methods. Columns, average of four wells. Data are representative of six separate experiments. **B.** Cells grown as in **A** were treated with 1 or 10 μmol/L imatinib and after 24 h, they were collected and subjected to cell cycle analysis by flow cytometry, as described in Materials and Methods. One representative of four similar experiments is shown here.

identified any subdiploid peak indicating, in accordance with the results from the viability assay (Fig. 1), that the effect of imatinib on human breast fibroblasts is cytostatic and not cytotoxic, at least at the concentrations tested.

Subsequently, we have investigated the effect of imatinib on the expression and activation of signaling molecules involved in the regulation of cell proliferation. First, we studied the activation of extracellular signal-regulated kinase (ERK) and Akt. Addition of different doses of imatinib (1 and 10 μmol/L) in proliferating cultures resulted in a dephosphorylation of both molecules (Fig. 3A). The effect on Akt was acute in both doses used, as a significant dephosphorylation was observed even 10 minutes after imatinib addition. On the other hand, the effect on ERK was more postponed. This is mainly due to the addition of the imatinib-containing solution that provokes a small activation of ERK, as was observed in control experiments

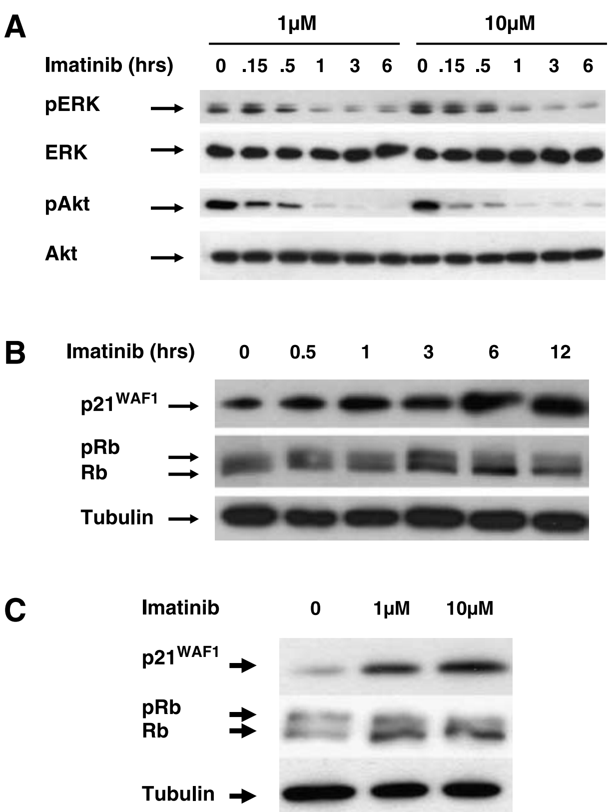

FIGURE 3. Effect of imatinib mesylate on the regulation of signaling pathways and cell cycle regulatory proteins in breast fibroblasts. **A.** In subconfluent fibroblast cultures, new serum-containing medium was added, and after 12 h, they were treated with imatinib (1 or 10 μmol/L). Subsequently, the cells were collected at the indicated time points and subjected to Western blot analysis by using antibodies against the phosphorylated forms of ERK and Akt. The expression of total ERK and Akt was used as loading controls. One representative of four identical experiments is shown here. **B.** Cells were grown as in **A** and treated with 10 μmol/L of imatinib. Total cellular protein was collected at the indicated time points and subjected to Western blot analysis by using antibodies against p21^{WAF1} and Rb. The latter recognizes the phosphorylated and unphosphorylated forms of the protein. Tubulin was used as a loading control. One representative of three separate experiments is shown. **C.** Cells were treated with 1 or 10 μmol/L of imatinib, collected 24 h later, and analyzed as in **B**.

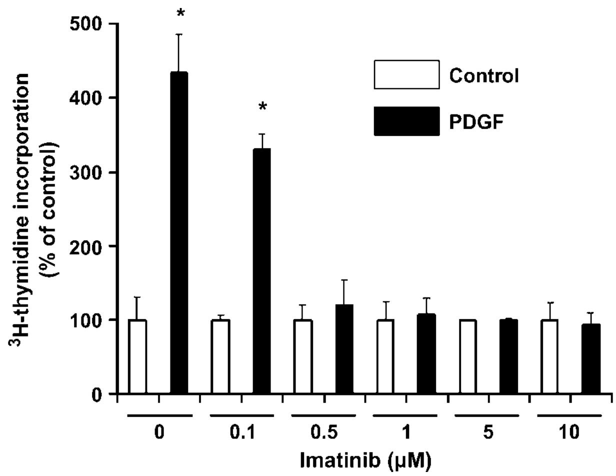

FIGURE 4. Imatinib mesylate inhibits the PDGF-mediated proliferation of breast fibroblasts. Confluent fibroblast cultures, arrested in DMEM containing 0.1% FCS, were preincubated for 60 min with the indicated imatinib concentrations and were then stimulated with PDGF (10 ng/mL). Twenty four hours later, DNA synthesis was estimated as described in Materials and Methods. Columns, average of four wells. Data are representative of three separate experiments. *, $P < 0.01$.

(not shown here), most probably via a shear stress effect. However, a significant dephosphorylation was observed at 30 minutes after imatinib addition and a more intense 1 hour after treatment. Then, we examined the downstream cell cycle regulators, i.e., the cyclin-dependent kinase inhibitor p21^{WAF1} and Rb protein that are involved in the control of G_1-S phase transition. As illustrated in Fig. 3B, at 6 and 12 hours after imatinib addition, a significant increase of p21^{WAF1} is observed, followed by the dephosphorylation of Rb. This is a dose-dependent effect, as can be seen in Fig. 3C, where the result of the treatment with 1 and 10 μmol/L imatinib is presented. Cumulatively, these data are in accordance with the arrest of fibroblast proliferation in the G_0/G_1 phase, as found by cell cycle analysis (Fig. 2B).

Imatinib-Mediated Inhibition of Fibroblast Proliferation Induced by PDGF

Next, we investigated the action of imatinib on the effect of PDGF on breast fibroblasts, having in mind that imatinib mesylate is a specific inhibitor of PDGF receptor. In subconfluent arrested fibroblast cultures, PDGF was found to strongly stimulate DNA synthesis, and this stimulation was blocked by imatinib in a dose-dependent manner (Fig. 4). Interestingly, this inhibition was more potent than that found in serum-containing cultures (Fig. 2A) as, at 0.5 μmol/L, a complete inhibition of DNA synthesis has been found. Imatinib was also found to inhibit the PDGF-mediated activation of MEK/ERK and phosphatidylinositol 3-kinase/Akt pathways (Fig. 5). To understand which pathway is crucial for the PDGF-mediated stimulation of proliferation and, thus, the inhibitory effect of imatinib, we used two specific inhibitors of these pathways, i.e., PD98059 (for the MEK/ERK pathway) and LY294002 (for the phosphatidylinositol 3-kinase/Akt pathway). As can be seen in Fig. 6, only LY294002 can effectively block

PDGF-mediated stimulation of DNA synthesis, suggesting that the inhibition of the Akt phosphorylation by imatinib may be responsible for its inhibitory effect. Similar results were obtained also with wortmannin, another phosphatidylinositol 3-kinase/Akt inhibitor (not shown).

The Effect of Imatinib on Collagen Synthesis by Human Breast Fibroblasts

Subsequently, we examined the effect of imatinib on collagen synthesis. By measuring [^{3}H]proline incorporation by the protease-free collagenase method, we have seen that imatinib can effectively inhibit novel collagen synthesis by breast fibroblasts (Fig. 7A). As the method used for measuring collagen synthesis cannot discriminate between the types of collagen synthesized and having in mind that collagen types I and III are overexpressed in breast carcinoma (29), we did quantitative PCR to examine the expression of *collagen types I* and *III*, and we have found that imatinib inhibits the expression of both genes after 6 and 24 hours of incubation (Fig. 7B). Finally, we have investigated the effect of imatinib on the expression of collagenases MMP-2 and MMP-9. To this end, we cultured the cells either on plastic surfaces or within gels of polymerized collagen, and after a 24-hour incubation in the absence or presence of imatinib, the conditioned media were subjected to gelatin zymography. As can be seen in Fig. 8, when cultured on plastic surfaces, breast fibroblasts secrete mainly pro–MMP-2, which is not affected by imatinib. These data were also confirmed by measuring gene expression by reverse transcription–PCR (data not shown). On the other hand, when cultured in collagen gels, breast fibroblasts secrete pro–MMP-9, pro–MMP-2, and activated MMP-2. Again the secreted proteases were found to be unaffected by imatinib. These data suggest that the inhibitory effect of imatinib on collagen synthesis is probably due to the direct inhibition of *collagen I* and *collagen III* transcription.

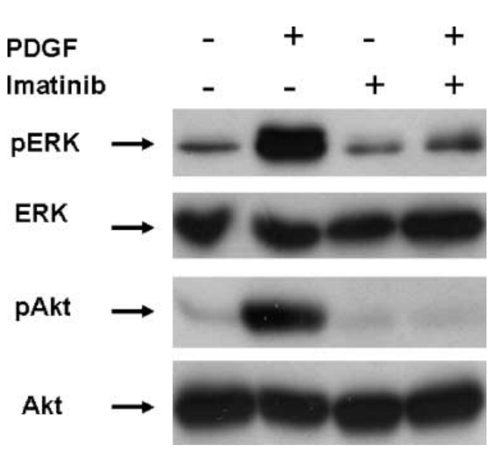

FIGURE 5. Imatinib mesylate inhibits PDGF-mediated ERK and Akt activation. Confluent breast fibroblast cultures, arrested in DMEM containing 0.1% FCS, were preincubated for 60 min with 10 μmol/L imatinib and were then stimulated with PDGF (10 ng/mL). After 30 min, the cells were collected and subjected to Western blot analysis by using antibodies against the phosphorylated forms of ERK and Akt. The expression of total ERK and Akt was used as loading controls. One representative of three identical experiments is shown here.

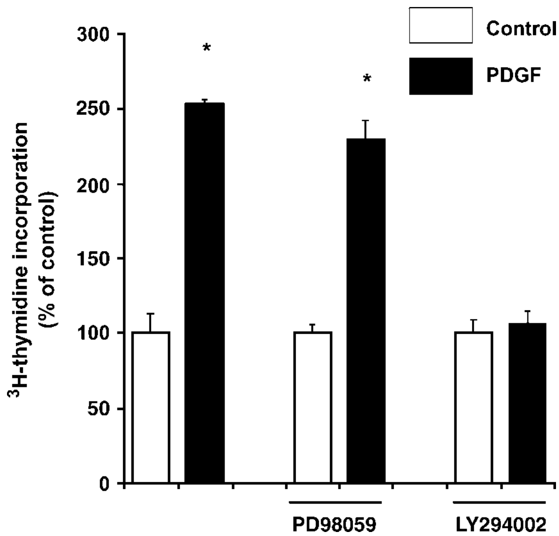

FIGURE 6. Effect of kinase inhibitors on PDGF-mediated breast fibroblast proliferation. Confluent fibroblast cultures, arrested in DMEM containing 0.1% FCS, were preincubated for 60 min with PD98059 (25 μmol/L) and LY294002 (10 μmol/L). Then PDGF (10 ng/mL) was added, and 24 h later, DNA synthesis was estimated as described in Materials and Methods. Columns, average of four wells. Data are representative of three separate experiments. *, $P < 0.01$.

Discussion

Recent studies have revealed the importance of tumor stroma in cancer cell growth, invasion, and metastatic progression (1, 13). In many human tumors, especially in the breast, the tumor microenvironment is essentially different from normal stroma, characterized by fibroblast proliferation, accompanied by an accumulation of extracellular matrix components, mainly collagen (2), a so-called "desmoplastic" reaction that exhibits synergistic effects on cancer growth (6). A crucial factor in the initiation of desmoplastic reaction is PDGF. Human breast cancer cells secrete PDGF ligands, whereas stromal fibroblasts express PDGF receptors and thus respond to these ligands in a paracrine manner (30-32). In addition, by using a xenograft model with breast cancer cells that express low-PDGF or high-PDGF levels, Shao and collaborators (2000) have shown that PDGF plays a prominent role in the initiation of this desmoplastic reaction. Accordingly, agents that can interfere with PDGF signaling may have an inhibitory effect on this stromal response and consequently on cancer growth. Imatinib mesylate (alternatively called Gleevec or Glivec or STI571) is an inhibitor of several protein kinases, i.e., c-Abl, c-Kit, and PDGF receptors (16). In addition, we have previously shown that imatinib can inhibit the growth and invasiveness of breast cancer epithelial cells (27, 28). So, based on the above, we have studied the effect of this drug on primary cultures of breast stromal fibroblasts. Our results have shown that imatinib exhibits an antifibrotic effect, as it inhibits the growth of these cells, as well as collagen production and secretion.

First, by studying the effect of imatinib on asynchronously growing fibroblast cultures, we have found that imatinib inhibits their proliferation with an IC_{50} of ~1 μmol/L (Fig. 2A). In contrast to results from cancer-associated fibroblasts from hepatic metastases of colorectal cancer (33),

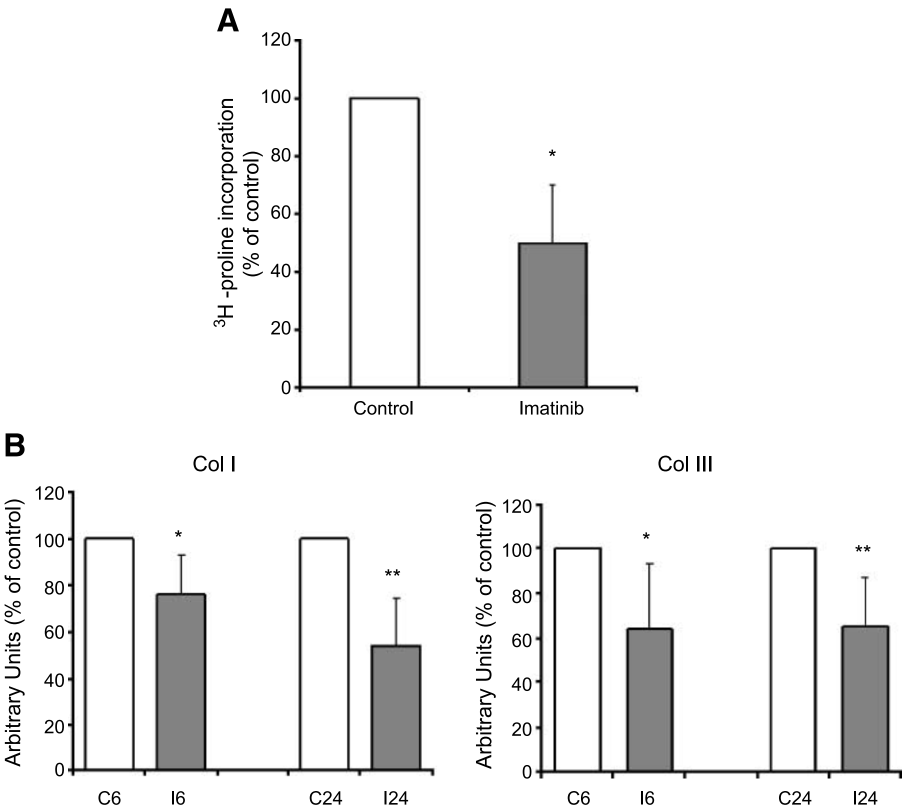

FIGURE 7. Imatinib mesylate inhibits collagen synthesis in human breast stromal fibroblasts. **A.** Confluent breast fibroblast cultures, arrested in DMEM containing 0.2% FCS in the presence of tritiated proline (5 μCi/mL), were treated with 10 μmol/L imatinib. Forty-eight hours later, collagen synthesis was estimated as described in Materials and Methods. Columns, average of eight separate experiments. **B.** Confluent breast fibroblast cultures, arrested in DMEM containing 0.2% FCS, were treated with 10 μmol/L imatinib. Cell lysates were collected at 6 and 24 h later in the absence (C6 and C24, respectively) or presence (I6 and I24, respectively) of imatinib, and RNA was isolated and subjected to real-time PCR, as described in Materials and Methods. Columns, average of three separate experiments. *, $P < 0.05$; **, $P < 0.01$.

the inhibitory effect of imatinib on breast cancer fibroblasts reported here is clearly cytostatic, as microscopic observations and results from a cytotoxicity assay (Fig. 1) have not shown any signs of cell death at concentrations up to 10 μmol/L.

To gain mechanistic insight into this inhibitory action, we have studied the effect of imatinib on the regulation of signaling molecules that are involved in cell proliferation. So, we have shown that it inhibits acutely and drastically serum-mediated and PDGF-mediated activation of the ERK and Akt pathways (Figs. 3A and 5). In addition, it up-regulates the expression of the cyclin-dependent kinase inhibitor $p21^{WAF1}$ and consequently leads to the dephosphorylation of the pRb protein (Figs. 3B and C). These effects are in agreement with the increase of the percentage of cells being in the G_0/G_1 phase of the cell cycle (Fig. 2B). Similarly, an increase of $p21^{WAF1}$ and a G_0/G_1 arrest after imatinib treatment has been reported for multiple myeloma cells (17). In contrast, in small cell lung and several anaplastic thyroid cancer cells, imatinib induces a G_2/M arrest (20, 21), thus suggesting a different regulation of signaling pathways.

Subsequently, we have also studied the action of imatinib on the PDGF-mediated DNA synthesis in human breast fibroblasts. PDGF stimulates DNA synthesis in these cells that is blocked by imatinib (Fig. 4). Interestingly, this inhibition is much more potent compared with that observed in fibroblasts grown in a serum-containing medium (Fig. 2A), as the growth potential of serum is not only due to PDGF but also due to other mitogens that probably activate separate signaling pathways that may not be inhibited by imatinib. Imatinib mesylate can also block PDGF-mediated ERK and Akt activation (Fig. 5). A partial or complete inhibition of these pathways have also been reported in several other normal and cancer cell lines (23, 24, 34-37), although this is not always the case (22). Although both pathways are involved in the regulation of proliferation in several cell types, by using specific inhibitors against these pathways (PD98059 for the MEK/ERK pathway and wortmannin or LY292004 for phosphatidylinositol 3-kinase/Akt), we have found that only the activation of Akt pathway is

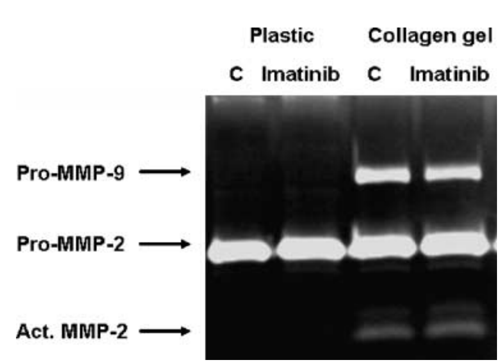

FIGURE 8. Imatinib mesylate does not alter gelatinase secretion and activation by human breast fibroblasts. Fibroblasts were grown to confluency on plastic cultures or within polymerized gels of type I collagen. Serum-free medium conditioned by these cultures in the presence or absence of 10 μmol/L imatinib was collected and subjected to gelatin zymography, as described in Materials and Methods. One representative of three similar experiments is presented here.

responsible for the transduction of the mitogenic effect of PDGF in breast fibroblasts and thus for the inhibitory action of imatinib on PDGF-mediated stimulation of DNA synthesis (Fig. 6).

As already mentioned, desmoplasia, i.e., the formation of an excessive dense connective tissue around the invasive tumor, is a characteristic of breast tumors. Interestingly, in benign breast lesions, types I and III collagen mRNAs are weakly expressed and their corresponding bundles are regularly organized, whereas in the stroma of malignant tumors, increased expression of these collagen types was observed in stromal fibroblastic cells and not in malignant epithelial cells (29). In addition, their expression is enhanced with increasing grades of malignancy, indicating that this may be linked with tumor invasion. Accordingly, we have studied the effect of imatinib on the synthesis and secretion of collagen by human breast stromal fibroblasts, and we have found, by using a tritiated proline incorporation assay, that it strongly inhibits the secretion of novel synthesized collagen (Fig. 7A). A similar effect of imatinib on the proliferation and collagen synthesis has been reported in rat cardiac fibroblasts (38). To further characterize this phenomenon in breast fibroblasts, we have shown, by using real-time PCR, a down-regulation of collagens I and III mRNA expression (Fig. 7B). In contrast, no alterations on MMP-2 and MMP-9 expression or activation were found by gelatin zymography (Fig. 8) or reverse transcription–PCR (not shown). Finally, reverse transcription–PCR studies have not revealed any alteration of MMP-1, TIMP-1, and TIMP-2 expression (data not shown). These findings are in agreement with previously reported data showing an antifibrotic effect of imatinib. In particular, it has been shown that it inhibits the mRNA expression of *α-smooth muscle actin* and *α2-(I)-procollagen* in rat hepatic stellate cells (35) and *α1-(I)-procollagen* and *α2-(I)-procollagen* in human dermal fibroblasts from normal and scleroderma donors (39). Interestingly, and in accordance with our data, in the latter study, no effect of imatinib on matrix metalloproteinases or tissue inhibitor of metalloproteinases was observed. However, in our study, no alteration in the expression of vimentin or α-smooth muscle actin was observed in breast stroma fibroblasts after incubation with different doses of imatinib from 0.1 to 10 μmol/L (not shown here). Finally, in *in vivo* studies, imatinib was found to inhibit experimentally induced dermal, lung, renal, and liver fibrosis by inhibiting the expression of collagen and other extracellular matrix proteins, e.g., fibronectin (35, 39-42).

Tumor interstitial hypertension has been documented in many tumors, including breast carcinoma (43), affecting drug delivery and penetration. In this direction, it has been shown that imatinib decreases interstitial fluid pressure in experimental tumors in immunocompromised mice and enhances the antitumor effect of Taxol (44). So, it seems that imatinib may affect breast carcinoma by multiple actions, i.e., (*a*) by decreasing interstitial fluid pressure, (*b*) by inhibiting the growth and invasiveness of breast cancers cells, and (*c*) by exerting an antifibrotic effect on breast stroma fibroblasts, as it inhibits both their proliferation and collagen synthesis, as shown here. Further *in vivo* studies are obviously required for the evaluation of its effectiveness in breast cancer treatment alone or in combination with other antitumor compounds.

Materials and Methods

Materials

Human recombinant PDGF-BB was purchased from R&D Systems. PD98059, wortmannin, and MTT were obtained from Sigma. Rabbit antibodies against tubulin, as well as goat anti-mouse and goat anti-rabbit horseradish peroxidase–conjugated secondary antibodies were obtained from Sigma. Rabbit anti–phosphorylated ERK1/2 (Thr^{202}/Tyr^{204}), anti–phosphorylated Akt (Ser^{473}), and anti-Akt antibodies were obtained from Cell Signaling Technology; mouse anti–pan-ERK and anti-$p21^{CIP1/WAF1}$ antibody from BD Transduction Laboratories. [^{3}H]Thymidine and L-[^{3}H]proline were from Amersham Biosciences. Imatinib mesylate was provided by Novartis Pharma AG. Crude collagenase and all cell culture media were purchased from Biochrom KG, whereas fetal bovine serum (FBS) was from Life Technologies Bethesda Research Laboratories.

Cells and Cell Culture Conditions

Primary cultures of human breast fibroblasts were developed from surgically removed cancer and adjacent normal breast tissue. The tissues were dissected and treated with crude type I collagenase (1 mg/mL), and after an overnight incubation, the cells were separated by centrifugation and cultured in DMEM, supplemented with penicillin-streptomycin, glutamine (all from Biochrom AG), and 10% FBS from Life Technologies Bethesda Research Laboratories (Invitrogen). Early passage cells were routinely subcultured when confluent by using a trypsin/citrate (0.25%:0.30% w/v) solution (45). The cells were maintained in a humidified atmosphere of 5% CO_2 at 37°C. They were also tested periodically and found to be *Mycoplasma*-free.

Cytotoxicity Assay

Cytotoxicity was estimated as previously described (46). In brief, human breast fibroblasts were plated in flat-bottomed 96-well microplates, in DMEM containing 10% FBS, until they reached confluency. Then, new medium was added, containing increasing concentrations of imatinib. After a 24-h, 48-h or 72-h incubation, the medium was replaced by MTT dissolved at a final concentration of 1 mg/mL in serum-free, phenol red–free medium. Then, MTT-formazan was solubilized in isopropanol, and absorbance was measured at a wavelength of 550 nm and a reference wavelenght of 690 nm.

DNA Synthesis Assay

Cells were plated at a density of $2 \times 10^4/cm^2$ in DMEM containing 10% FBS, and when grown to ~80% confluency, new medium was added along with increasing concentrations of imatinib and [methyl-^{3}H]thymidine (0.15 μCi/mL, 25 Ci/mmol). After 24 h of incubation, the culture medium was aspirated and the cells were washed with PBS, fixed with 10% ice-cold trichloroacetic acid, washed extensively under running tap water, and air-dried. DNA was solubilized by the addition of 0.3 N NaOH/1% SDS, and the lysates were subjected to scintillation counting, as previously described (47). Alternatively, the cells were grown until confluency and were then rendered quiescent after a 48-h period in DMEM supplemented with 0.1% FBS. Then, new medium was added with increasing concentrations of imatinib along with [methyl-^{3}H]thymidine, and DNA synthesis was estimated as above. Finally, in the experiments with PDGF, confluent quiescent cultures were preincubated with increasing concentrations of imatinib, and 60 min later, PDGF was added. Twenty-four hours later, DNA synthesis was estimated as described above.

Cell Cycle Analysis

Cell cycle analysis was done by flow cytometry, as previously described (48). Cells were plated sparsely in DMEM containing 10% FBS. When still subconfluent, the cultures were treated with imatinib (1 or 10 μmol/L), and after a 24-h period, the cells were trypsinized, washed with PBS, fixed in 50% (v/v) ethanol, and stained with propidium iodide (50 μg/mL) in the presence of $MgCl_2$ (5 mmol/L) and Rnase A (10 μg/mL) in Tris-HCl (pH 7.5; 10 mmol/L). DNA content was analyzed on a FACSCalibur flow cytometer (Becton Dickinson) using the Modfit software.

Western Blot Analysis

Subconfluent cultures of human breast fibroblasts, proliferating in DMEM supplemented with 10% FBS, were treated with the indicated doses of imatinib for various time periods. At the indicated time points, the cells were washed with ice-cold PBS, lysed into 2× hot SDS-PAGE sample buffer [125 mmol/L Tris-HCl (pH 6.8), 5% (w/v) SDS, 20% (v/v) glycerol, 125 mmol/L β-mercaptoethanol, 0.02% (w/v) bromophenol blue, supplemented with protease and phosphatase inhibitors (Sigma)], boiled for 5 min, sonicated for 15 s, clarified by centrifugation, and stored at −80°C until use. The lysates were separated on SDS-PAGE, and the proteins were transferred to polyvinylidene difluoride membranes (Amersham Biosciences). The membranes were blocked with 5% w/v nonfat dried milk in 1 mmol/L Tris-HCl (pH 7.4), 150 mmol/L NaCl, 0.05% Tween 20 (TTBS) buffer and incubated with the appropriate primary antibodies. After washing with TTBS, the membranes were incubated with the respective second antibody for 1 h and washed again with TTBS, and the immunoreactive bands were visualized on Kodak-X-OMAT AR film by enhanced chemiluminescence kit according to the manufacturer's (Amersham Biosciences) instructions. The intensity of the bands was quantified after capture with a CCD camera connected to a personal computer, using the BioProfil image analysis software (Vilber Lourmat). Alternatively, confluent quiescent fibroblast cultures (in DMEM supplemented with 0.1% FBS; see DNA synthesis above) were pretreated with imatinib (10 μmol/L); 60 min later, they were stimulated with PDGF-BB (10 ng/mL) and the cells were collected as above.

Quantitative Reverse Transcription–PCR Analysis

Total RNA from the samples was extracted using TRIzol reagent (Invitrogen). First-strand cDNA was synthesized from 1 μg of total RNA with the help of an oligo(dT) primer, using Moloney murine leukemia virus reverse transcriptase (Invitrogen). Quantitative PCR was done using Mx3000P qPCR system and MxPro Version 3.00 software (Stratagene), with the help of the Brilliant SYBR Green qPCR Master Mix kit (Stratagene), in a total volume of 25 μL. The sequences of the primers used are shown in Table 1. Amplification conditions consisted of initial denaturation at 95°C for 10 min, followed by 40 cycles of denaturation at 95°C for 30 s, annealing at 61°C (COL3, β-actin) or 56°C (COL1, β-actin) for 60 s, and elongation at 72°C for 30 s. Melting curve analysis and electrophoresis on 3% agarose gels were done to ensure that the expected PCR products were generated. To quantify specific mRNA in the samples, a standard curve was produced for each run based on four points from diluted cDNA, whereas a nontemplate control was always included. All experiments were repeated at least thrice. Relative mRNA expression levels for each sample were calculated as the ratio of the specific mRNA copy number for each mRNA species under evaluation to the β-actin mRNA copy number, thus normalizing mRNA expression of each gene tested for sample-to-sample differences in RNA input, quality, and reverse transcriptase efficiency.

Collagen Synthesis

Collagen synthesis was measured by a modification of the protease-free collagenase method (49). Fibroblast cultures after reaching confluency were cultured for 24 h in DMEM containing 0.1% FCS. The medium was then removed, and cultures were supplemented with fresh medium containing 5 μCi/mL L-[^{3}H]proline (26 mCi/mmol), βAPN (50 μg/mL), and ascorbic acid (50 μg/mL) in the presence or absence of imatinib and incubated for 48 h. Then the medium was precipitated with trichloroacetic acid (final concentration, 10%). The resulting pellet was dissolved in 0.2 N NaOH, and one half of each sample was digested with protease-free collagenase from *Clostridium histoliticum* [EC number 3.4.24.3 (from Sigma), 5 BTC units/mL of buffer containing 0.005 N $CaCl_2$ and 0.2 N NaCl, 0.05 mol/L Tris-HCl (pH 7.4)] for 2 h at 37°C and 16 h at room temperature; subsequently, the undigested protein was precipitated with trichloroacetic acid. After centrifugation, the supernatant and one wash were collected, and radioactivity was measured in a β-counter. Collagen synthesis of each sample was calculated by subtracting the

Table 1. QPCR Primer Sequences

Name	Sequence	Genbank code no.	Length of PCR product
COL1-F	CCA GAA GAA CTG GTA CAT CA	NM_000088	96
COL1-R	CCG CCA TAC TCG AAC TGG AA		
COL3-F	GGA CCT GCT GGA CCA AAT GG	NM_000090	137
COL3-R	CCC CTC ATT CCT GGA CCT CC		
β-Actin F	TTG GCA ATG AGC GGT TCC	NM_001101	148
β-Actin R	AGC ACT GTG TTG GCG TAC		

radioactivity of the blank (untreated half of the sample) from the radioactivity of the collagenase-treated half, and this was finally normalized according to the number of cells in culture.

Collagen Extraction—Preparation of Collagen Gels

Collagen was extracted from rat tail tendons, as previously described (50). Briefly, tendons were solubilized in 0.1% (v/v) acetic acid for 48 h at 4°C. The solution was filtered, dialyzed against DMEM 0.1× for 48 h at 4°C, sterilized by filtration, and stored at 4°C. This stock solution contains ∼2.5 mg/mL total protein and consists primarily of collagen type I. Collagen gels were prepared by mixing the above collagen stock solution with sodium bicarbonate (0.15 mol/L) and DMEM 10× at a ratio of 8:2:1; the mixture was supplemented with FCS at a final concentration of 0.1%. Two milliliters from this solution were placed into each 35-mm dish and left for at least 30 min at 37°C for polymerization. DMEM (2 mL) supplemented with 0.1% FCS was overlaid after gelation.

Conditioned Media

Media conditioned by human breast fibroblasts, cultured on plastic or in three-dimensional collagen gels, were collected as follows. (*a*) On plastic, confluent fibroblast cultures on plastic dishes were washed (3×) with DMEM and then incubated with serum-free DMEM, in the presence or absence of imatinib (10 μmol/L) for 24 h. At the end of the incubation period, the serum-free conditioned medium was collected, centrifuged for 30 min at $10^4 \times g$ to clarify it from cell debris, and stored at −80°C. (*b*) The cells were seeded within collagen gels in DMEM supplemented with 0.1% FCS. After 36 h, the cells were washed as above and then incubated with serum-free DMEM, the presence or absence of imatinib (10 μmol/L), for 24 h. Serum-free conditioned medium was collected as above.

Zymography

Gelatin zymography was done as described previously (38). Conditioned media were separated under nonreducing conditions on 10% SDS-polyacrylamide gels, impregnated with 1 mg/mL gelatin. After electrophoresis, SDS was eluted from the gels by shaking in a buffer [5 mmol/L $CaCl_2$, 50 mmol/L Tris-HCl (pH 7.4)] containing 2.5% Triton-X-100, 3 × 20 min, at room temperature. The gels were then incubated for 40 h at 37°C in a substrate buffer [5 mmol/L $CaCl_2$, 50 mmol/L Tris-HCl (pH 7.4)]. The gels were stained with Coomasie Brilliant Blue R250, and gelatin-degrading enzymes were identified as clear bands against a blue background. The intensity of the bands was quantified after capture with a CCD camera connected to a personal computer, using the BioProfil image analysis software (Vilber Lourmat).

Statistics

Data were analyzed by using the *t* test. Differences between mean values were statistically significant for $P < 0.01$ or $P < 0.05$, as indicated in the figures.

Disclosure of Potential Conflicts of Interest

No potential conflicts of interest were disclosed.

Acknowledgments

We thank Novartis Pharma AG for providing imatinib mesylate and Dr. Elisabeth Buchdunger for critically reviewing the manuscript.

References

1. Micke P, Ostman A. Tumour-stroma interaction: cancer-associated fibroblasts as novel targets in anti-cancer therapy? Lung Cancer 2004;45 Suppl 2:S163–75.

2. Noel A, Foidart JM. The role of stroma in breast carcinoma growth *in vivo*. J Mammary Gland Biol Neoplasia 1998;3:215–25.

3. Tlsty TD, Hein PW. Know thy neighbor: stromal cells can contribute oncogenic signals. Curr Opin Genet Dev 2001;11:54–9.

4. Orimo A, Weinberg RA. Stromal fibroblasts in cancer: a novel tumor-promoting cell type. Cell Cycle 2006;5:1597–601.

5. Walker RA. The complexities of breast cancer desmoplasia. Breast Cancer Res 2001;3:143–5.

6. Shao ZM, Nguyen M, Barsky SH. Human breast carcinoma desmoplasia is PDGF initiated. Oncogene 2000;19:4337–45.

7. Cardone A, Tolino A, Zarcone R, Borruto Caracciolo G, Tartaglia E. Prognostic value of desmoplastic reaction and lymphocytic infiltration in the management of breast cancer. Panminerva Med 1997;39:174–7.

8. Maeshima AM, Niki T, Maeshima A, Yamada T, Kondo H, Matsuno Y. Modified scar grade: a prognostic indicator in small peripheral lung adenocarcinoma. Cancer 2002;95:2546–54.

9. Allinen M, Beroukhim R, Cai L, et al. Molecular characterization of the tumor microenvironment in breast cancer. Cancer Cell 2004;6:17–32.

10. Ronnov-Jessen L, Petersen OW, Koteliansky VE, Bissell MJ. The origin of the myofibroblasts in breast cancer. Recapitulation of tumor environment in culture unravels diversity and implicates converted fibroblasts and recruited smooth muscle cells. J Clin Invest 1995;95:859–73.

11. Chauhan H, Abraham A, Phillips JR, Pringle JH, Walker RA, Jones JL. There is more than one kind of myofibroblast: analysis of CD34 expression in benign, *in situ*, and invasive breast lesions. J Clin Pathol 2003;56:271–6.

12. Petersen OW, Nielsen HL, Gudjonsson T, et al. Epithelial to mesenchymal transition in human breast cancer can provide a nonmalignant stroma. Am J Pathol 2003;162:391–402.

13. Bhowmick NA, Neilson EG, Moses HL. Stromal fibroblasts in cancer initiation and progression. Nature 2004;432:332–7.

14. Barcellos-Hoff MH, Ravani SA. Irradiated mammary gland stroma promotes the expression of tumorigenic potential by unirradiated epithelial cells. Cancer Res 2000;60:1254–60.

15. Coussens LM, Werb Z. Inflammation and cancer. Nature 2002;420:860–7.

16. Roskoski R, Jr. STI-571: an anticancer protein-tyrosine kinase inhibitor. Biochem Biophys Res Commun 2003;309:709–17.

17. Pandiella A, Carvajal-Vergara X, Tabera S, Mateo G, Gutierrez N, San Miguel JF. Imatinib mesylate (STI571) inhibits multiple myeloma cell proliferation and potentiates the effect of common antimyeloma agents. Br J Haematol 2003;123:858–68.

18. Zhang P, Gao WY, Turner S, Ducatman BS. Gleevec (STI-571) inhibits lung cancer cell growth (A549) and potentiates the cisplatin effect *in vitro*. Mol Cancer 2003;2:1.

19. Krystal GW, Honsawek S, Litz J, Buchdunger E. The selective tyrosine kinase inhibitor STI571 inhibits small cell lung cancer growth. Clin Cancer Res 2000;6:3319–26.

20. Wang WL, Healy ME, Sattler M, et al. Growth inhibition and modulation of kinase pathways of small cell lung cancer cell lines by the novel tyrosine kinase inhibitor STI 571. Oncogene 2000;19:3521–8.

21. Podtcheko A, Ohtsuru A, Tsuda S, et al. The selective tyrosine kinase inhibitor, STI571, inhibits growth of anaplastic thyroid cancer cells. J Clin Endocrinol Metab 2003;88:1889–96.

22. Li J, Kleeff J, Guo J, et al. Effects of STI571 (gleevec) on pancreatic cancer cell growth. Mol Cancer 2003;2:32.

23. McGary EC, Weber K, Mills L, et al. Inhibition of platelet-derived growth factor-mediated proliferation of osteosarcoma cells by the novel tyrosine kinase inhibitor STI571. Clin Cancer Res 2002;8:3584–91.

24. Matei D, Chang DD, Jeng MH. Imatinib mesylate (Gleevec) inhibits ovarian cancer cell growth through a mechanism dependent on platelet-derived growth factor receptor α and Akt inactivation. Clin Cancer Res 2004;10:681–90.

25. Joensuu H, Roberts PJ, Sarlomo-Rikala M, et al. Effect of the tyrosine kinase inhibitor STI571 in a patient with a metastatic gastrointestinal stromal tumor. N Engl J Med 2001;344:1052–6.

26. Verweij J, Judson I, van Oosterom A. STI571: a magic bullet? Eur J Cancer 2001;37:1816–9.

27. Roussidis AE, Mitropoulou TN, Theocharis AD, et al. STI571 as a potent inhibitor of growth and invasiveness of human epithelial breast cancer cells. Anticancer Res 2004;24:1445–7.

28. Roussidis AE, Theocharis AD, Tzanakakis GN, Karamanos NK. The importance of c-Kit and PDGF receptors as potential targets for molecular therapy in breast cancer. Curr Med Chem 2007;14:735–43.

29. Kauppila S, Stenback F, Risteli J, Jukkola A, Risteli L. Aberrant type I and type III collagen gene expression in human breast cancer *in vivo*. J Pathol 1998; 186:262–8.

30. de Jong JS, van Diest PJ, van der Valk P, Baak JP. Expression of growth factors, growth inhibiting factors, and their receptors in invasive breast cancer: I. An inventory in search of autocrine and paracrine loops. J Pathol 1998;184: 44–52.

31. Sariban E, Sitaras NM, Antoniades HN, Kufe DW, Pantazis P. Expression of platelet-derived growth factor (PDGF)-related transcripts and synthesis of biologically active PDGF-like proteins by human malignant epithelial cell lines. J Clin Invest 1988;82:1157–64.

32. Lindmark G, Sundberg C, Glimelius B, Pahlman L, Rubin K, Gerdin B. Stromal expression of platelet-derived growth factor β-receptor and platelet-derived growth factor B-chain in colorectal cancer. Lab Invest 1993;69:682–9.

33. Mueller L, Goumas FA, Himpel S, Brilloff S, Rogiers X, Broering DC. Imatinib mesylate inhibits proliferation and modulates cytokine expression of human cancer-associated stromal fibroblasts from colorectal metastases. Cancer Lett 2007;250:329–38.

34. Sanz-Gonzalez SM, Castro C, Perez P, Andres V. Role of E2F and ERK1/2 in STI571-mediated smooth muscle cell growth arrest and cyclin A transcriptional repression. Biochem Biophys Res Commun 2004;317:972–9.

35. Yoshiji H, Noguchi R, Kuriyama S, et al. Imatinib mesylate (STI-571) attenuates liver fibrosis development in rats. Am J Physiol Gastrointest Liver Physiol 2005;288:G907–13.

36. Li L, Blumenthal DK, Masaki T, Terry CM, Cheung AK. Differential effects of imatinib on PDGF-induced proliferation and PDGF receptor signaling in human arterial and venous smooth muscle cells. J Cell Biochem 2006;99: 1553–63.

37. Appel S, Rupf A, Weck MM, et al. Effects of imatinib on monocyte-derived dendritic cells are mediated by inhibition of nuclear factor-κB and Akt signaling pathways. Clin Cancer Res 2005;11:1928–40.

38. Schellings MW, Baumann M, van Leeuwen RE, et al. Imatinib attenuates end-organ damage in hypertensive homozygous TGR(mRen2)27 rats. Hypertension 2006;47:467–74.

39. Distler JH, Jungel A, Huber LC, et al. Imatinib mesylate reduces production of extracellular matrix and prevents development of experimental dermal fibrosis. Arthritis Rheum 2007;56:311–22.

40. Aono Y, Nishioka Y, Inayama M, et al. Imatinib as a novel antifibrotic agent in bleomycin-induced pulmonary fibrosis in mice. Am J Respir Crit Care Med 2005;171:1279–85.

41. Daniels CE, Wilkes MC, Edens M, et al. Imatinib mesylate inhibits the profibrogenic activity of TGF-β and prevents bleomycin-mediated lung fibrosis. J Clin Invest 2004;114:1308–16.

42. Wang S, Wilkes MC, Leof EB, Hirschberg R. Imatinib mesylate blocks a non-Smad TGF-β pathway and reduces renal fibrogenesis *in vivo*. FASEB J 2005; 19:1–11.

43. Less JR, Posner MC, Boucher Y, Borochovitz D, Wolmark N, Jain RK. Interstitial hypertension in human breast and colorectal tumors. Cancer Res 1992; 52:6371–4.

44. Pietras K, Rubin K, Sjoblom T, et al. Inhibition of PDGF receptor signaling in tumor stroma enhances antitumor effect of chemotherapy. Cancer Res 2002;62: 5476–84.

45. Kletsas D, Stathakos D. Quiescence and proliferative response of normal human embryonic fibroblasts in homologous environment. Effect of aging. Cell Biol Int Rep 1992;16:103–13.

46. Gioka C, Bourauel C, Hiskia A, Kletsas D, Eliades T, Eliades G. Light-cured or chemically cured orthodontic adhesive resins? A selection based on the degree of cure, monomer leaching, and cytotoxicity. Am J Orthod Dentofacial Orthop 2005;127:413–9; quiz 516.

47. Kletsas D, Stathakos D, Sorrentino V, Philipson L. The growth-inhibitory block of TGF-β is located close to the G1/S border in the cell cycle. Exp Cell Res 1995;217:477–83.

48. Giannouli CC, Kletsas D. TGF-β regulates differentially the proliferation of fetal and adult human skin fibroblasts via the activation of PKA and the autocrine action of FGF-2. Cell Signal 2006;18:1417–29.

49. Zervolea I, Pratsinis H, Tsagarakis S, et al. The impact of chronic *in vivo* glucocorticoid excess on the functional characteristics of human skin fibroblasts obtained from patients with endogenous Cushing's syndrome. Eur J Endocrinol 2005;152:895–902.

50. Zervolea I, Kletsas D, Stathakos D. Autocrine regulation of proliferation and extracellular matrix homeostasis in human fibroblasts. Biochem Biophys Res Commun 2000;276:785–90.